The promyelocytic leukemia zinc finger gene, *PLZF*, is frequently downregulated in malignant mesothelioma cells and contributes to cell survival

Mitchell Cheung[1,*], **Jianming Pei**[1,*], **Yaguang Pei**[1], **Suresh C. Jhanwar**[2], **Harvey I. Pass**[3], and **Joseph R. Testa**[1]

[1]Cancer Genetics and Signaling Program, Fox Chase Cancer Center, Philadelphia, PA, USA

[2]Department of Pathology, Memorial Sloan-Kettering Cancer Center, New York, NY, USA

[3]Department of Cardiothoracic Surgery, New York University School of Medicine, New York, NY, USA

Abstract

DNA copy number analysis was performed, using SNP mapping arrays, to fine map genomic imbalances in human malignant mesothelioma (MM) cell lines derived from primary tumors. Chromosomal losses accounted for the majority of genomic imbalances. All 22 cell lines examined showed homozygous deletions of 9p21.3, centering at the *CDKN2A/ARF* and *CDKN2B* loci. Other commonly underrepresented segments included 1p36, 1p22, 3p21-22, 4q13, 4q34, 11q23, 13q12-13, 14q32, 15q15, 18q12 and 22q12, each observed in 55%–90% of cell lines. Focal deletions of 11q23 encompassed the transcriptional repressor gene *PLZF* (promyelocytic leukemia zinc finger), which was validated by analysis of genomic DNA using real-time PCR. Semi-quantitative RT-PCR and immunoblot analysis revealed that PLZF is greatly downregulated in MM cell lines compared to non-malignant mesothelial cells. Ectopic expression of PLZF in PLZF-deficient MM cells resulted in decreased cell viability, reduced colony formation, as well as increased apoptosis, the latter based on results of various cell death assays and the observation of increased cleavage of caspase 3, PARP and Mcl-1. These data indicate that deletions of *PLZF* are a common occurrence in MM and that downregulation of PLZF may contribute to MM pathogenesis by promoting cell survival.

Keywords

mesothelioma; *PLZF*; genomic imbalances; tumor suppressors; transcription factor

---

Correspondence: Dr Joseph R. Testa; Cancer Genetics and Signaling Program, Fox Chase Cancer Center, 333 Cottman Avenue, Philadelphia, PA 19111-2497, USA. Joseph.Testa@fccc.edu.
*MC and JP contributed equally to this work.

Conflict of interest

The authors declare no conflict of interest.

Introduction

Malignant mesothelioma (MM) is a highly aggressive form of cancer that arises from the serosal lining of the pleural, peritoneal, and pericardial cavities. Epidemiological studies have established that exposure to asbestos fibers is the primary cause of MM (Craighead and Mossman, 1982; Wagner *et al.*, 1960). In the USA, ~2,500 cases of MM are diagnosed annually, and the incidence of this disease is expected to increase over the next two decades due to past occupational exposure to asbestos. MM is characterized by a long latency, typically 20–40 years, from the time of asbestos exposure to diagnosis, suggesting that multiple, cumulative somatic genetic changes are required for the tumorigenic conversion of a mesothelial cell. Cytogenetic studies have uncovered numerous clonal chromosomal alterations in most MMs (reviewed in (Murthy and Testa, 1999). Prominent among these changes are recurrent deletions of discrete segments within chromosome arms 1p, 3p, 6q, 9p, 13q and 15q; losses of chromosomes 4 and 22 are also frequently observed. Many of these recurrent genomic imbalances can occur in combination in a given tumor, suggestive of a multistep pathogenetic process. Subsequent deletion mapping investigations have revealed that discrete chromosomal segments, e.g., 1p22, 3p21, 9p21 and 22q12, show high frequencies of allelic loss in MM tumor specimens and derived tumor cell lines (Murthy and Testa, 1999). To date, tumor suppressor genes at two sites of recurrent chromosomal loss have been implicated in MM: *CDKN2A/ARF* and *CDKN2B*, which are located at 9p21, and *NF2*, which resides at 22q12 (Altomare *et al.*, 2005; Cheng *et al.*, 1999).

The recent availability of microarray-based platforms designed to detect recurring copy number abnormalities (CNAs) at a high-resolution, genome-wide level has facilitated the discovery of tumor suppressor genes and oncogenes involved in various cancers (Greshock *et al.*, 2007). In this investigation, single nucleotide polymorphism (SNP)-based microarrays were used to detect multiple recurrent sites of chromosomal loss, including several novel regions, in tumor cell lines derived from 22 primary MMs. One of these sites, 11q23, encompassed the transcriptional repressor gene *PLZF* (promyelocytic leukemia zinc finger), which was shown to be greatly downregulated in MM cell lines. Experimental re-expression of PLZF resulted in decreased colony formation and increased apoptosis, suggesting that downregulation of PLZF may contribute to MM pathogenesis by promoting cell survival.

Results

DNA copy number analysis reveals multiple sites of recurrent genomic imbalance in MM cell lines, particularly chromosomal losses

DNA copy number analysis was performed on 22 human MM cell lines. Figure 1A depicts a DNA copy number analysis profile of the entire genome of a representative cell line. All cell lines exhibited multiple genomic imbalances, and a schematic summary of CNAs observed in the entire set of cell lines is shown in Figure 1B. Chromosomal losses were more common than gains. All cell lines showed losses of 9p21.3. In many lines, there was a pronounced loss of signal for multiple contiguous markers in 9p21.3 surrounded by a larger region with a lesser loss of signal, a pattern indicative of a homozygous deletion embedded within a heterozygous deletion (Pei *et al.*, 2006). Such a pattern suggests the existence of two different but overlapping interstitial losses of 9p. A summary of all losses of chromosome 9

in the entire cell line panel is shown in Figure 1B. Notably, all 22 cell lines showed homozygous deletions of 9p21.3, centering at the *CDKN2A/ARF* and *CDKN2B* loci. At the location of the nearby *MTAP* locus, thought to encode another tumor suppressor, there were no SNPs; however, at the next SNP proximal to the *CDKN2A/ARF* locus, homozygous losses were detected in 100% of cell lines.

Other commonly underrepresented sites were located in sub-bands 1p36.2-36.3 (55%), 1p22.1-22.3 (82%), 3p22.1-p21.31 (77%), 11q23.2-23.3 (64%), 13q12.2-13.2 (73%), 14q32.2 (73%), 15q15.1 (55%), and 18q12.3 (59%). In addition to small deletions, whole chromosome loss or deletion of a very large portion of chromosomes 22 and 4 were observed in 78% and 53% of MM cell lines, respectively, with peak levels of loss at 4q13.1, 4q34.1 and 22q12.1-12.2 being observed in 82%–90% of the cell lines.

Genomic gains were generally less common than losses, although a gain of 17q23.2 was observed in 55% of the samples. While some striking examples of genomic amplification were observed in individual MM cell lines (e.g., see Figure 1A), recurrent sites of amplification were not identified. The 3p amplicon shown in Figure 1A is notable in that the boundary between the amplified segment and a deletion resided within the *FHIT* gene located at a fragile site in 3p14.2 (data not shown). The breakpoint causes deletion of *FHIT* exons 2 to 5 and amplification of exon 1.

Recurrent chromosomal losses at 11q23 encompass the transcriptional repressor gene, PLZF, a putative tumor suppressor gene

Our attention was drawn to 11q23.2-23.3, because we had not noted the extent of loss in this region in MM based on chromosomal analyses with lower resolution methodologies, i.e., karyotyping and metaphase-CGH analysis (Balsara *et al.*, 1999; Taguchi *et al.*, 1993). Moreover, we identified overlapping focal deletions in 11q23.2 in several cell lines (Figure 2A), with deletions consistently encompassing the *PLZF* (promyelocytic leukemia zinc finger) gene, which has previously been implicated in human malignancy (Felicetti *et al.*, 2004; McConnell and Licht, 2007; Shiraishi *et al.*, 2007). Furthermore, 11 of our 22 MM cell lines showed predicted LOH in the 11q region encompassing the *PLZF* gene, based on Affymetrix allele analysis. Real-time quantitative PCR analysis of genomic DNA validated the hemizygous deletion of *PLZF* (data not shown).

PLZL is frequently downregulated in MM cells and restoration of PLZF expression results in decreased cell viability, reduced colony formation, and increased apoptosis

Furthermore, semi-quantitative RT-PCR indicated that *PLZF* was greatly downregulated in MM cell lines compared to the expression observed in non-malignant mesothelial cells (Figure 2B, *upper panel*). Downregulation was observed in MM lines with deletions detected by DNA copy number analysis as well as in several other cell lines without obvious deletions at the *PLZF* locus, suggesting that gene silencing occurs in some MM cell lines. Downregulation of PLZF in MM cell lines was confirmed by Western blot analysis (Figure 2B, *lower panel*).

To gain insights regarding the potential role of downregulation of PLZF in MM, we initially transfected several MM cell lines with a PLZF expression construct, which resulted in diminished cell viability, based on an MTS assay (Figure 3A). We next carried out a clonogenic assay in which several PLZF-deficient MM cell lines were transfected with a PLZF expression construct or the empty vector. Ectopic expression of PLZF consistently resulted in a greatly decreased number of colonies compared to cells transfected with empty vector (Figure 3B). Re-expression of PLZF did not result in cell cycle arrest (Supplemental Figure 1). However, ectopic expression of PLZF in MM cells resulted in an increase in the number of apoptotic floating cells, which was confirmed by a DNA fragmentation ELISA assay (Figure 4A) and by an increase in the sub-G1 cellular fraction observed by flow cytometry analysis (Figure 4B). Expression of PLZF resulted in an increase in the Mcl-1 cleaved protein (Mcl-1*), which is detected as a ~30 kDa band (Snowden *et al.*, 2003; Michels *et al.*, 2004) (Figure 4C). The Mcl-1 cleaved protein has been demonstrated to have a pro-apoptotic function, in contrast to the pro-survival full length Mcl-1 protein (Michels *et al.*, 2004). Collectively, these data suggest that loss of PLZF expression plays a role in promoting the survival of MM cells.

Discussion

The precise mapping of recurrent somatic changes in DNA copy number, a hallmark of the cancer genome, has facilitated the discovery of novel tumor suppressor genes and oncogenes (Greshock *et al.*, 2007). Microarray-based platforms have proven to be of particular utility in this regard, because they permit high-resolution, genome-wide detection of CNAs in a high-throughput manner. To identify frequent CNAs in MM, we used SNP-based mapping arrays to perform DNA copy number analysis of 22 human MM cell lines derived from primary tumors.

This analysis showed multiple aberrations in all cell lines, a feature consistent with previous cytogenetic studies of tumor specimens and cell lines from MM patients (reviewed in (Murthy and Testa, 1999; Musti *et al.*, 2006). Collectively, these findings suggest that genomic instability is a hallmark of MM. Among the many CNAs observed, a discrete set of highly recurrent genomic imbalances is obvious (Figure 1B). Most of the recurrent CNAs represent deletions, suggesting that losses of tumor suppressor genes play a key role in the pathogenesis of MM. The fine mapping of recurrent CNAs highlight a number of chromosomal sites where known or putative tumor suppressor genes reside.

Prominent among the sites of recurring chromosomal loss is 9p21.3, which encompasses the *CDKN2A/ARF* and *CDKN2B* tumor suppressor genes. The *CDKN2A/ARF* locus encodes p16(INK4A) and p14(ARF), respectively, two proteins that regulate critical cell cycle regulatory pathways. The p16(INK4A) product is a cyclin-dependent kinase inhibitor that regulates the RB1 pathway, whereas p14(ARF) regulates the p53 pathway via binding to the p53-stabilizing protein MDM2.

In earlier PCR-based deletion mapping studies, we identified homozygous deletions of *p16(INK4A)* in 34 of 40 (85%) human MM cell lines tested (Cheng *et al.*, 1994), and in subsequent work, we documented homozygous deletions of part or all of *p14(ARF)* in 36 of

these 40 (90%) cell lines, with co-deletion of *p16(INK4A)* and *p14(ARF)* in most instances (Altomare *et al.*, 2005). Functional studies demonstrated that re-expression of p16(INK4A) in MM cells results in cell cycle arrest, cell death, tumor suppression and tumor regression (Frizelle *et al.*, 1998). In addition, re-expression of p14(ARF) in cultured human MM cell lines has been shown to induce G1-phase cell cycle arrest and apoptotic cell death (Yang *et al.*, 2000), suggesting that *p14(ARF)*, like *p16(INK4A)*, is an important target of 9p21 deletions in MM.

The deletions of 9p21.3 seen in the present study also consistently result in homozygous loss of *CDKN2B*, encoding the cyclin-dependent kinase inhibitor p15(INK4B). To date, a critical role for loss of *CDKN2B* in MM has not been clearly defined. The methylthioadenosine phosphorylase gene (*MTAP*) was also frequently co-deleted with the *CDKN2A/ARF* and *CDKN2B* loci in MM, and its role as a tumor suppressor gene has been proposed (Christopher *et al.*, 2002). This is consistent with a study by Illei et al., in which 64 of 70 (91%) primary MM tumor specimens with homozygous deletions of *p16(INK4A)* exhibited co-deletion of *MTAP* (Illei *et al.*, 2003).

In a previous metaphase-CGH analysis on human MM cell lines, we reported recurrent losses of 1p12–22, 13q12–14, 14q24–qter, 6q25–qter, 9p21, 15q11.1–21 and 22q, each with a frequency of 38–58% (Balsara *et al.*, 1999). The lower incidence and less precise nature of the findings with metaphase-CGH analysis is a reflection of its limited mapping resolution (3–10 Mb). The much higher resolution possible with microarray-based mapping chips (median intermarker distance = 17Kb for the 50K chip) permitted us to precisely identify small common regions of overlapping genomic loss or gain with various chromosomes. Moreover, the microarray-based studies revealed several novel regions of chromosomal loss, including sub-bands 11q23.2-23.3, 1p36.2-36.3, and 18q12.3 pinpointing the sites of putative tumor suppressor genes that may play a role in the pathogenesis of MM. *PLZF*, located at 11q23.2-23.3, was pursued because this gene has previously been implicated in other human malignancies.

The PLZF transcriptional repressor gene was initially identified as the fusion partner of the retinoic acid receptor-alpha gene, *RARA*, in a patient with acute promyelocytic leukemia and a translocation t(11;17)(q23;21) (Chen *et al.*, 1993; McConnell and Licht, 2007). Chen et al. cloned cDNAs encoding PLZF-RARA chimeric proteins and examined their transactivating activities in retinoic acid-sensitive myeloid cells (Chen *et al.*, 1994). A dominant-negative effect was observed when PLZF-RARA fusion proteins were co-transfected with vectors expressing RARA and retinoid X receptor alpha, RXRA, and thus implicated the fusion proteins in the molecular pathogenesis of APL.

Expression of PLZF has also been shown to be downregulated in melanomas compared to normal melanocytes (Felicetti *et al.*, 2004). Retroviral-mediated expression of PLZF has been shown to inhibit the *in vitro* migration and invasiveness of melanoma cells, consistent with a less malignant phenotype, and this was confirmed by *in vivo* studies performed in athymic nude mice (Felicetti *et al.*, 2004). Furthermore, expression profiling revealed that PLZF-transduced melanoma cells exhibited a more differentiated, melanocyte-like pattern, thus suggesting a suppressor role for PLZF in solid tumors.

PLZF protein has been described as a transcriptional repressor of homeobox (HOX)-containing genes during embryogenesis. Barna *et al.* generated *Plzf* –/– mice and showed that *Plzf* is essential for patterning of the limb and axial skeleton by acting as a mediator of anterior-to-posterior patterning in both the axial and appendicular skeleton (Barna *et al.*, 2002). They demonstrated that inactivation of the *Plzf* gene resulted in patterning defects affecting all skeletal structures of the limb, and that Plzf acts as a growth-inhibitory and proapoptotic factor in the limb bud.

We found that re-expression of PLZF in PLZF-deficient MM cells inhibits clonogenic growth and acts to promote apoptosis. The cleavage of Mcl-1 into the ~30 kDa Mcl-1 fragment may be important downstream effect of the caspase signaling cascade. Michels et al. demonstrated that expression of cleaved Mcl-1 results in increase cell death (Michels *et al.*, 2004). Ectopic expression of PLZF has also been shown to promote apoptosis in other types of human cancer cells including cervical carcinoma cells (Rho *et al.*, 2007) and Jurkat T-cell leukemia cells (Bernardo *et al.*, 2007). Microarray expression analysis of stable Jurkat clones with inducible expression of PLZF revealed that the apoptosis-inducer *TP53INP1*, *ID1*, and *ID3* genes were upregulated, and that the apoptosis-inhibitor *TERT* (telomerase reverse transcriptase) gene was downregulated (Bernardo *et al.*, 2007). However, our RT-PCR analysis did not detect changes in the expression of these genes in MM cells transfected with PLZF (data not shown). Furthermore, immunoblot analysis revealed no change in TP53INP1 protein level nor changes in the expression of various BH3 family members tested, such as Bcl-xL, Bax, PUMA or NOXA (Figure 4C).

MYC and the cyclin A gene (*CCNA2*) have also been reported as PLZF target genes (McConnell *et al.*, 2003; Yeyati *et al.*, 1999). However, ectopic expression of PLZF in MM cell lines did not result in decreased expression of MYC or cyclin A, nor did we observe cell cycle arrest. Other investigators have also failed to see a connection between expression of PLZF and that of MYC and/or cyclin A (Costoya *et al.*, 2004; Felicetti *et al.*, 2004). Moreover, it should be noted that up regulation of MYC or cyclin A may not be essential to promote cell proliferation in MM cell lines, because they consistently exhibit homozygous deletions of the *CDKN2A* gene, which encodes an inhibitor of cyclin-dependent kinases.

In summary, the DNA copy number analysis presented here demonstrates that MM cells harbor numerous recurrent genomic imbalances, particularly deletions targeting sites of known or putative tumor suppressor loci such as *CDKN2A/ARF*. In addition to previously reported sites of chromosomal loss characteristic of MM, other recurrent novel sites of chromosomal loss are apparent including deletions of 11q23.2, where the *PLZF* gene resides. Our findings indicate that downregulation of PLZF is a common occurrence in MM cells and may contribute to pathogenesis of MM by promoting cell survival.

Materials and methods

Tumor cell lines

Tumor cell lines were established from surgically resected human MM specimens as described elsewhere (Taguchi *et al.*, 1993). All MM cases were newly diagnosed, previously untreated patients. As controls, we used LP9 (AG07086, from Coriell Institute, Camden, NJ,

USA), a primary human mesothelial cell strain, and LP9/TERT-1, which are hTERT-immortalized, non-tumorigenic LP9 cells (Dickson *et al.*, 2000).

DNA copy number analysis

Genomic DNA was isolated using a Qiagen Gentra Puregene DNA isolation kit (Qiagen, Valencia, CA, USA). Human Mapping 50K Array *Xba* 240 GeneChips (Affymetrix, Santa Clara, CA, USA) containing approximately 59,000 SNPs were used as hybridization targets. The array probe datasheet can be found at http://www.affymetrix.com/products/arrays/specific/100k.affx. Total genomic DNA (250 ng) from each tumor cell line was digested with *Xba*I restriction enzyme and ligated to an adapter that recognizes cohesive 4-basepair (bp) overhangs. Then a generic primer that specifically recognizes the adapter sequence was used to amplify the adapter-ligated DNA fragments. The polymerase chain reaction (PCR) conditions were optimized to preferentially amplify fragments in the 250–2,000-bp size range. Following purification, amplified DNA was fragmented with DNase I, biotin-labeled, and then hybridized to GeneChips in an Affymetrix Hybridization Oven 640. Washing and staining of the arrays were performed with an Affymetrix Fluidics Station 450, and images were obtained using an Affymetrix GeneChip 7G Scanner 3000 according to the manufacturer's recommendations. Probe hybridization intensities were analyzed with Affymetrix software GCOS 1.4, and genotyping was performed using GTYPE 4.1 with Dynamic Model Mapping Analysis by default settings (0.25) for both homozygote and heterozygote call thresholds. Copy number analyses were carried out using the Affymetrix Chromosome Copy Number Analysis Tool (CNAT) 4.0 with a genomic smoothing window setting of 0.1 Mb and a reference data set of 128 samples including 42 from African Americans, 20 from East Asians (10 Chinese, 10 Japanese), 42 from Caucasians, and 24 from the Affymetrix Polymorphism Discovery (PD) Panel. Peak frequencies of CNAs were scored based on the average incidence of genomic gain or loss at 3 or more contiguous SNPs.

Real-time quantitative PCR of genomic DNA copy number

Primers located within exon 2 of the *PLZF* gene were designed to quantitate *PLZF* genomic DNA copy number in MM cell lines using real-time PCR. The forward primer was 5'-AGA GCC CTT CAG TCT CCA CTT C-3' and the reverse primer was 5'-AGG AGA GAC TGT CCT ATG GTC ATC A-3'. The sequence of the fluorigenic BlackHole1 probe was 5'-FAM-TCT TTC AGC CAT GAG TCC CAC CAA G-BHQ1-3'.

Semi-quantitative reverse transcriptase-PCR (RT-PCR)

Total RNA was isolated from subconfluent MM cell lines using Trizol (Invitrogen, Carlsbad, CA, USA). First strand cDNA was synthesized with Superscript II and Oligo dT (both from Invitrogen). Primer 3 (http://frodo.wi.mit.edu/cgi-bin/primer3/primer3_www.cgi) was used to design gene specific primer pairs within open reading frames but excluding regions of high homology with related gene members (after BLAST analysis) or repetitive elements (Repeatmasker, http://www.repeatmasker.org/cgi-bin/WEBRepeatMasker). The primers used to amplify *PLZF*, CACACAGGCAGACCCATACT and TTTGTGGCTCTTGAGTGTGC, are located within two different exons to prevent

contaminating genomic DNA amplification. The cDNA was amplified in a multiplex PCR reaction with *GAPDH* primers (GAGTCAACGGATTTGGTCGT and TTCTAGACGGCAGGTCAGGT) using AmpliTaq Gold (Applied Biosystems, Foster City, CA, USA) and analyzed in a 2% agarose gel.

Cell proliferation and clonogenic assays

PLZF cDNA expression construct in pcDNA6 (cat. # SC116350) was obtained from Origene (Rockville, MD, USA). MM cell lines were transfected with Amaxa Nucleofector reagent R, program G-16 (PPM-Con, PPM-Mill), program A-20 (PPM-Rob), or program A-23 (PPM-Phi). After overnight recovery, 3000 cells/well (PPM-Rob), 2000 cells/well (PPM-Con, PPM-Phi), or 1000 cells/well (PPM-Mill) were plated onto 96-well plates in replicates of 8. Cell number was determined using the CellTiter 96 AQueous Assay (Promega, Madison, WI, USA) after *in vitro* culture for 72 hours.

The *PLZF* cDNA expression construct was directionally subcloned into pcDNA3.1(−)puro plasmid after the *PLZF* cDNA was amplified using primers containing flanking *Eco*RI and *Xho*I sites. Construct inserts were sequence verified. The cell lines were transfected with 1.45 pmol of pcDNA3.1puro empty plasmid, pcDNA3.1puro PLZF, or pcDNA3.1Hygro (non-puromycin resistant control plasmid) using Amaxa Nucleofector reagent R and the appropriate program previously mentioned. After transfection, 2.4×10^5 cells (PPM-Rob and PPM-Mill), 3.6×10^5 cells (PPM-Phi), or 1×10^6 cells (PPM-Con) were plated onto 6-well plates in triplicate. The following day, the media was replaced with media containing puromycin (0.4 μg/ml for PPM-Rob, 0.5 μg/ml for PPM-Mill, and 0.3 μg/ml for PPM-Con and PPM-Phi). Fresh media containing puromycin was added every 2 days during the 7-day selection. After selection, the cells were washed with PBS, fixed in 4% paraformaldehyde for 10 min, and then rinsed with water. The cells were stained with 0.05% crystal violet (dissolved in 10% ethanol) for 30 min and then rinsed three times with water before air drying. The number of colonies, consisting of 20 or more cells, in triplicate wells were counted to generate survival curves. All experiments were repeated at least three times, with similar results.

Cell Cycle Analysis

Attached transfected cells were washed with PBS and harvested with trypsin. The cells were spun down at $1000 \times g$ and the pellet washed with cold PBS. After a second centrifugation, the cells were resuspended in 200 μl of cold PBS. The cell suspension was added dropwise into a tube containing 4 ml of cold 70% ethanol while gently vortexing and allowed to fix at 4°C overnight or longer. Cells were stained with 40 μg/ml propidium iodide (Sigma, St. Louis, MO, USA) and treated with RNase A (Sigma) for 30 min at room temperature before analyzing by flow cytometry using a FACscan cell analyzer (BD Biosciences, San Jose, CA, USA) equipped with Cellquest software (BD Biosciences) and analyzed using FlowJo software (Tree Star, Ashland, OR).

In Vitro Detection of Apoptosis

24 or 48 hours after transfection, floating and attached cells were collected for DNA fragmentation detection using a Cell Death Detection ELISA Plus Kit (Roche Diagnostics,

Mannheim, Germany) by following the manufacturer's suggested protocol. Detection of sub-G1 apoptotic cells was performed by collecting floating and attached cells for cell cycle analysis as described in the previous section.

Western blot analysis

Cells were harvested, and lysates were prepared with 1X Cell Lysis Buffer (Cell Signaling Technology, Danvers, MA, USA) supplemented with 1 mM PMSF (Sigma, St. Louis, MO, USA). For the transfection experiments, both floating cells and cells attached to the plate were pooled to prepare cell lysates. Protein was quantitated using the Bradford method (Bio-Rad Laboratories, Hercules, CA, USA), resolved on a NuPAGE Bis-Tris gel (Invitrogen), and transferred onto PVDF membrane. PLZF antibodies ab38739 and sc-28319 were from Abcam (Cambridge, MA, USA) and Santa Cruz Biotechnology (Santa Cruz, CA, USA), respectively. GAPDH (sc-32233) antibody was from Santa Cruz Biotechnology; NOXA (IMG-349A) was obtained from Imgenex (San Diego, CA, USA), and TP53INP1 (#905-300) was acquired from Assay Designs (Ann Arbor, MI, USA). Caspase 3 (#9662), PARP (#9542), Mcl-1 (#4572), Bcl-xL (#2764), p53 (#2527), phospho-p53 (ser46) (#2521), BAX (#2772), BAD (#9292), phospho-BAD (ser112) (#9296), BIM (#2819), PUMA (#4976), BID (#2002), and BIK (#4592) antibodies were from Cell Signaling Technology.

Supplementary Material

Refer to Web version on PubMed Central for supplementary material.

Acknowledgements

References

Altomare DA, Vaslet CA, Skele KL, De Rienzo A, Devarajan K, Jhanwar SC, et al. A mouse model recapitulating molecular features of human mesothelioma. Cancer Res. 2005; 65:8090–8095. [PubMed: 16166281]

Balsara BR, Bell DW, Sonoda G, De Rienzo A, du Manoir S, Jhanwar S, et al. Comparative genomic hybridization and loss of heterozygosity analyses identify a common region of deletion at 15q11.1-15 in human malignant mesothelioma. Cancer Res. 1999; 59:450–454. [PubMed: 9927061]

Barna M, Merghoub T, Costoya JA, Ruggero D, Branford M, Bergia A, et al. Plzf mediates transcriptional repression of HoxD gene expression through chromatin remodeling. Dev Cell. 2002; 3:499–510. [PubMed: 12408802]

Bernardo MV, Yelo E, Gimeno L, Campillo JA, Parrado A. Identification of apoptosis-related PLZF target genes. Biochem Biophys Res Commun. 2007; 359:317–322. [PubMed: 17537403]

Chen S-J, Zelent A, Tong J-H, Yu H-Q, Wang Z-Y, Derre J, et al. Rearrangements of the retinoic acid receptor alpha and promyelocytic leukemia zinc finger genes resulting from t(11;17)(q23;q21) in a patient with acute promyelocytic leukemia. J Clin Invest. 1993; 91:2260–2267. [PubMed: 8387545]

Chen Z, Guidez F, Rousselot P, Agadir A, Chen S-J, Wang Z-Y, et al. PLZF-RAR-alpha fusion proteins generated from the variant t(11;17)(q23;q21) translocation in acute promyelocytic leukemia

inhibit ligand-dependent transactivation of wild-type retinoic acid receptors. Proc Natl Acad Sci USA. 1994; 91:1178–1182. [PubMed: 8302850]

Cheng JQ, Jhanwar SC, Klein WM, Bell DW, Lee W-C, Altomare DA, et al. *p16* alterations and deletion mapping of 9p21-p22 in malignant mesothelioma. Cancer Res. 1994; 54:5547–5551. [PubMed: 7923195]

Cheng JQ, Lee WC, Klein MA, Cheng GZ, Jhanwar SC, Testa JR. Frequent mutations of NF2 and allelic loss from chromosome band 22q12 in malignant mesothelioma: evidence for a two-hit mechanism of NF2 inactivation. Genes Chromosomes Cancer. 1999; 24:238–242. [PubMed: 10451704]

Christopher SA, Diegelman P, Porter CW, Kruger WD. Methylthioadenosine phosphorylase, a gene frequently codeleted with p16(cdkN2a/ARF), acts as a tumor suppressor in a breast cancer cell line. Cancer Res. 2002; 62:6639–6644. [PubMed: 12438261]

Costoya JA, Hobbs RM, Barna M, Cattoretti G, Manova K, Sukhwani M, et al. Essential role of Plzf in maintenance of spermatogonial stem cells. Nat Genet. 2004; 36:653–659. [PubMed: 15156143]

Craighead JE, Mossman BT. The pathogenesis of asbestos-associated diseases. N. Engl. J. Med. 1982; 306:1446–1455. [PubMed: 7043267]

Dickson MA, Hahn WC, Ino Y, Ronfard V, Wu JY, Weinberg RA, et al. Human keratinocytes that express hTERT and also bypass a p16(INK4a)-enforced mechanism that limits life span become immortal yet retain normal growth and differentiation characteristics. Mol Cell Biol. 2000; 20:1436–1447. [PubMed: 10648628]

Felicetti F, Bottero L, Felli N, Mattia G, Labbaye C, Alvino E, et al. Role of PLZF in melanoma progression. Oncogene. 2004; 23:4567–4576. [PubMed: 15077196]

Frizelle SP, Grim J, Zhou J, Gupta P, Curiel DT, Geradts J, et al. Re-expression of p16INK4a in mesothelioma cells results in cell cycle arrest, cell death, tumor suppression and tumor regression. Oncogene. 1998; 16:3087–3095. [PubMed: 9671387]

Greshock J, Feng B, Nogueira C, Ivanova E, Perna I, Nathanson K, et al. A comparison of DNA copy number profiling platforms. Cancer Res. 2007; 67:10173–10180. [PubMed: 17968032]

Illei PB, Rusch VW, Zakowski MF, Ladanyi M. Homozygous deletion of CDKN2A and codeletion of the methylthioadenosine phosphorylase gene in the majority of pleural mesotheliomas. Clin Cancer Res. 2003; 9:2108–2113. [PubMed: 12796375]

McConnell MJ, Chevallier N, Berkofsky-Fessler W, Giltnane JM, Malani RB, Staudt LM, et al. Growth suppression by acute promyelocytic leukemia-associated protein PLZF is mediated by repression of c-myc expression. Mol Cell Biol. 2003; 23:9375–9388. [PubMed: 14645547]

McConnell MJ, Licht JD. The PLZF gene of t (11;17)-associated APL. Curr Top Microbiol Immunol. 2007; 313:31–48. [PubMed: 17217037]

Michels J, O'Neill JW, Dallman CL, Mouzakiti A, Habens F, Brimmell M, et al. Mcl-1 is required for Akata6 B-lymphoma cell survival and is converted to a cell death molecule by efficient caspase-mediated cleavage. Oncogene. 2004; 23:4818–4827. [PubMed: 15122313]

Murthy SS, Testa JR. Asbestos, chromosomal deletions, and tumor suppressor gene alterations in human malignant mesothelioma. J Cell Physiol. 1999; 180:150–157. [PubMed: 10395284]

Musti M, Kettunen E, Dragonieri S, Lindholm P, Cavone D, Serio G, et al. Cytogenetic and molecular genetic changes in malignant mesothelioma. Cancer Genet. Cytogenet. 2006; 170:9–15. [PubMed: 16965949]

Pei J, Kruger WD, Testa JR. High-resolution analysis of 9p loss in human cancer cells using single nucleotide polymorphism-based mapping arrays. Cancer Genet Cytogenet. 2006; 170:65–68. [PubMed: 16965958]

Rho SB, Chung BM, Lee JH. TIMP-1 regulates cell proliferation by interacting with the ninth zinc finger domain of PLZF. J Cell Biochem. 2007; 101:57–67. [PubMed: 17340613]

Shiraishi K, Yamasaki K, Nanba D, Inoue H, Hanakawa Y, Shirakata Y, et al. Pre-B-cell leukemia transcription factor 1 is a major target of promyelocytic leukemia zinc-finger-mediated melanoma cell growth suppression. Oncogene. 2007; 26:339–348. [PubMed: 16862184]

Snowden RT, Sun XM, Dyer MJ, Cohen GM. Bisindolylmaleimide IX is a potent inducer of apoptosis in chronic lymphocytic leukaemic cells and activates cleavage of Mcl-1. Leukemia. 2003; 17:1981–1989. [PubMed: 14513048]

Taguchi T, Jhanwar SC, Siegfried JM, Keller SM, Testa JR. Recurrent deletions of specific chromosomal sites in 1p, 3p, 6q, and 9p in human malignant mesothelioma. Cancer Res. 1993; 53:4349–4355. [PubMed: 8364929]

Wagner JC, Sleggs CA, Marchand P. Diffuse pleural mesotheliomas and asbestos exposure in the northwestern cape province. Br J Ind Med. 1960; 12:260–271. [PubMed: 13782506]

Yang CT, You L, Yeh CC, Chang JW, Zhang F, McCormick F, et al. Adenovirus-mediated p14(ARF) gene transfer in human mesothelioma cells. J Natl Cancer Inst. 2000; 92:636–641. [PubMed: 10772681]

Yeyati PL, Shaknovich R, Boterashvili S, Li J, Ball HJ, Waxman S, et al. Leukemia translocation protein PLZF inhibits cell growth and expression of cyclin A. Oncogene. 1999; 18:925–934. [PubMed: 10023668]

Figure 1A
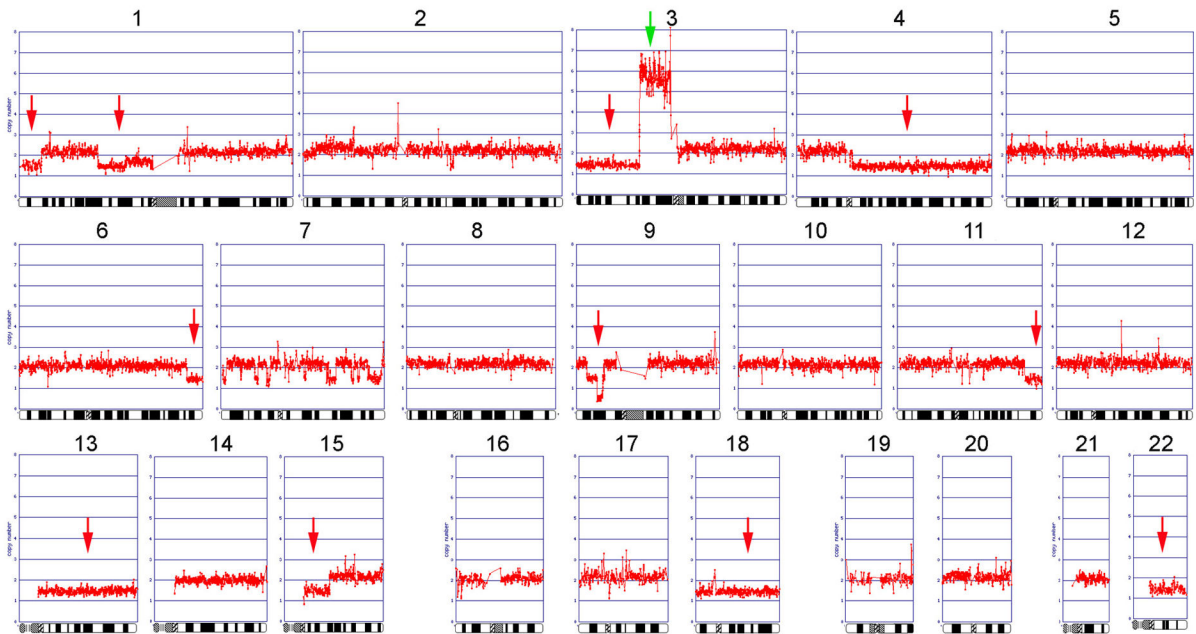
Figure 1B
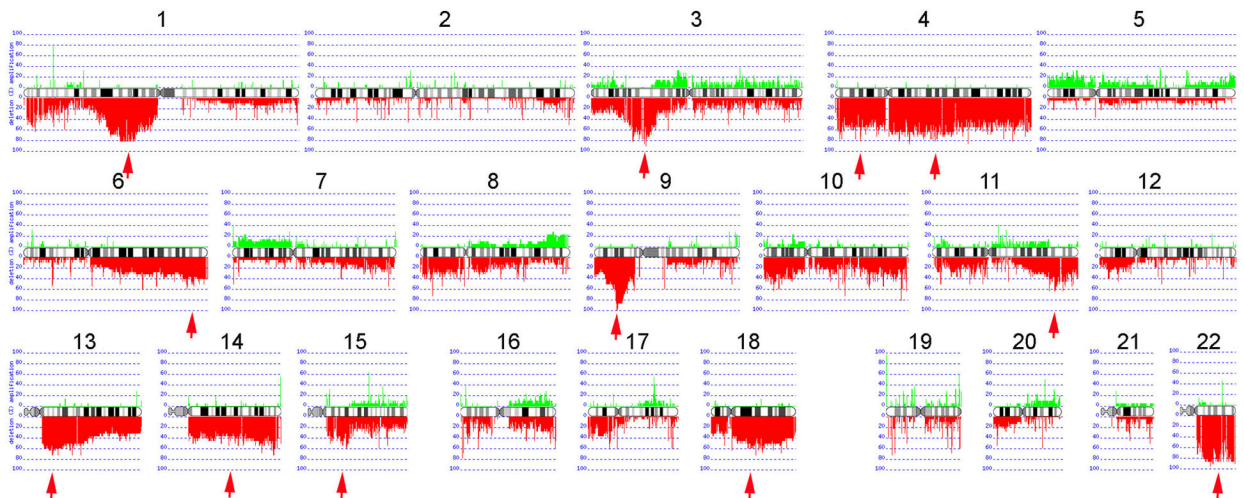
Figure 1.
A) DNA copy number analysis profile of the entire genome of a representative MM cell line showing multiple alterations, including nearly all of the recurrent chromosomal deletions (red arrows) seen in the overall series. The 3p amplicon (green arrow) is notable in that the boundary between the proximal amplified segment and the more distal deletion resides within the FHIT gene located at a fragile site in 3p14.2. *B)* Schematic summary of CNAs observed in the entire set of MM cell lines highlighting common regions of copy number losses (red arrows) in multiple chromosomes, including 1p, 3p, 4p/q, 6q, 9p, 11q, 13q, 14q,

15q, 18q, and 22q. Note that all 22 cell lines showed homozygous deletions of 9p21.3, centering at the *CDKN2A/ARF* and *CDKN2B* loci.
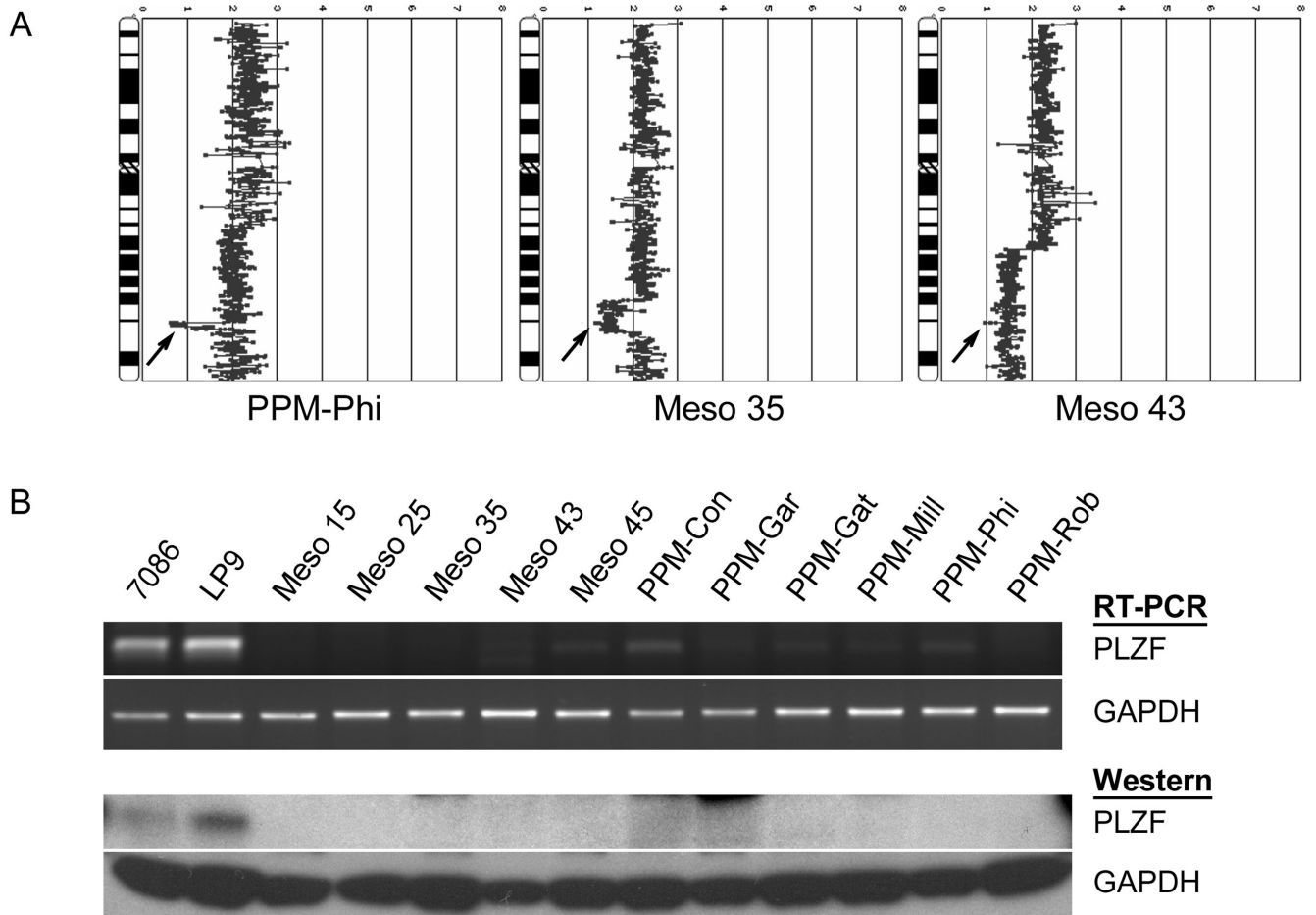
Figure 2.
A) DNA copy number analysis profiles of chromosome 11 in three MM cell lines. Losses overlap in 11q23.2-23.3, including one cell line with a focal deletion encompassing the *PLZF* gene. *B) Upper panel*: Semi-quantitative RT-PCR showing downregulation of *PLZF* in 11 MM cell lines compared to the expression observed in control mesothelial cells, LP9 and LP9/TERT-1. *Lower panel*: Immunoblot analysis demonstrating downregulation of PLZF protein in MM cells compared to control mesothelial cells.
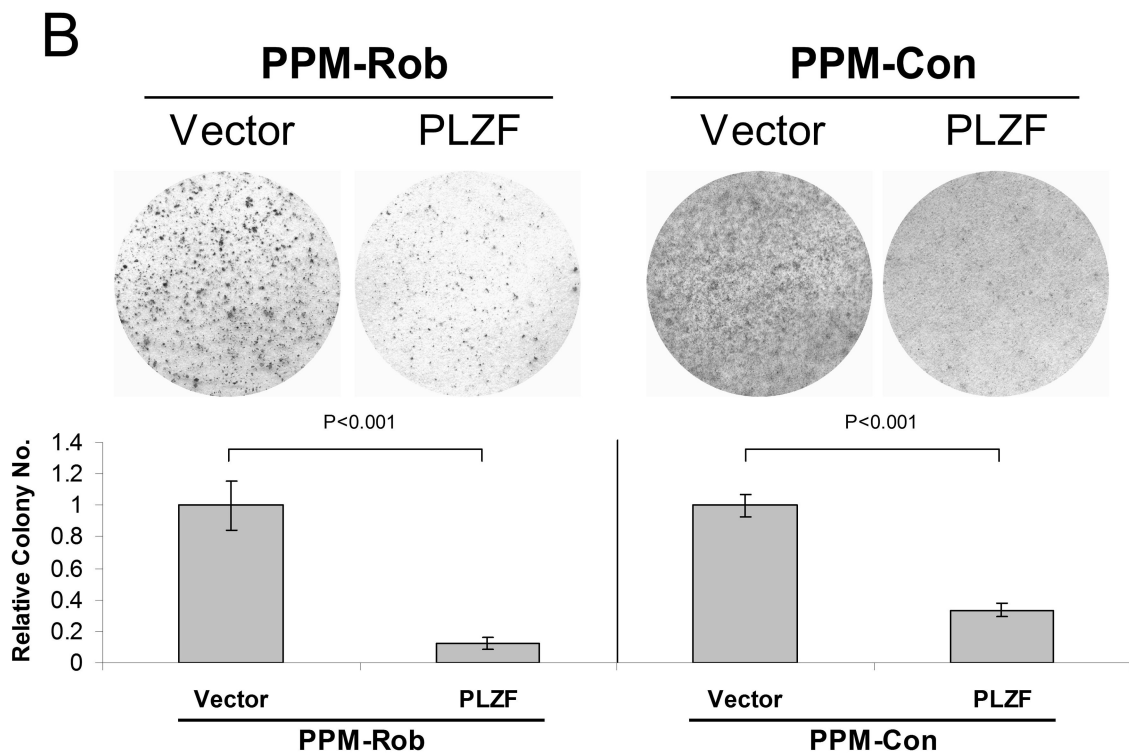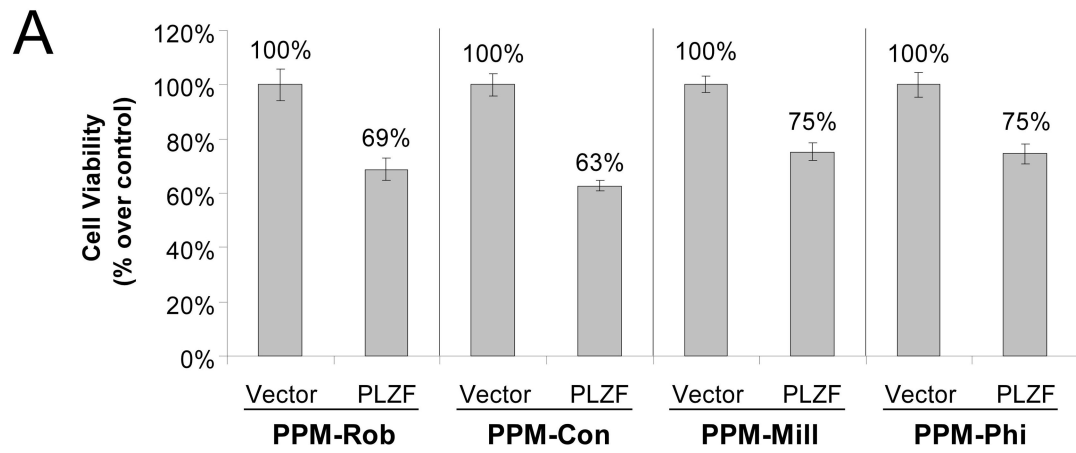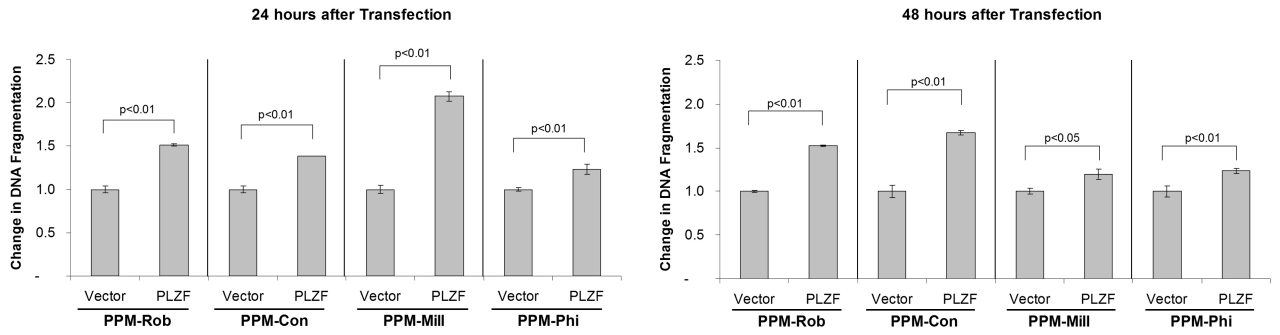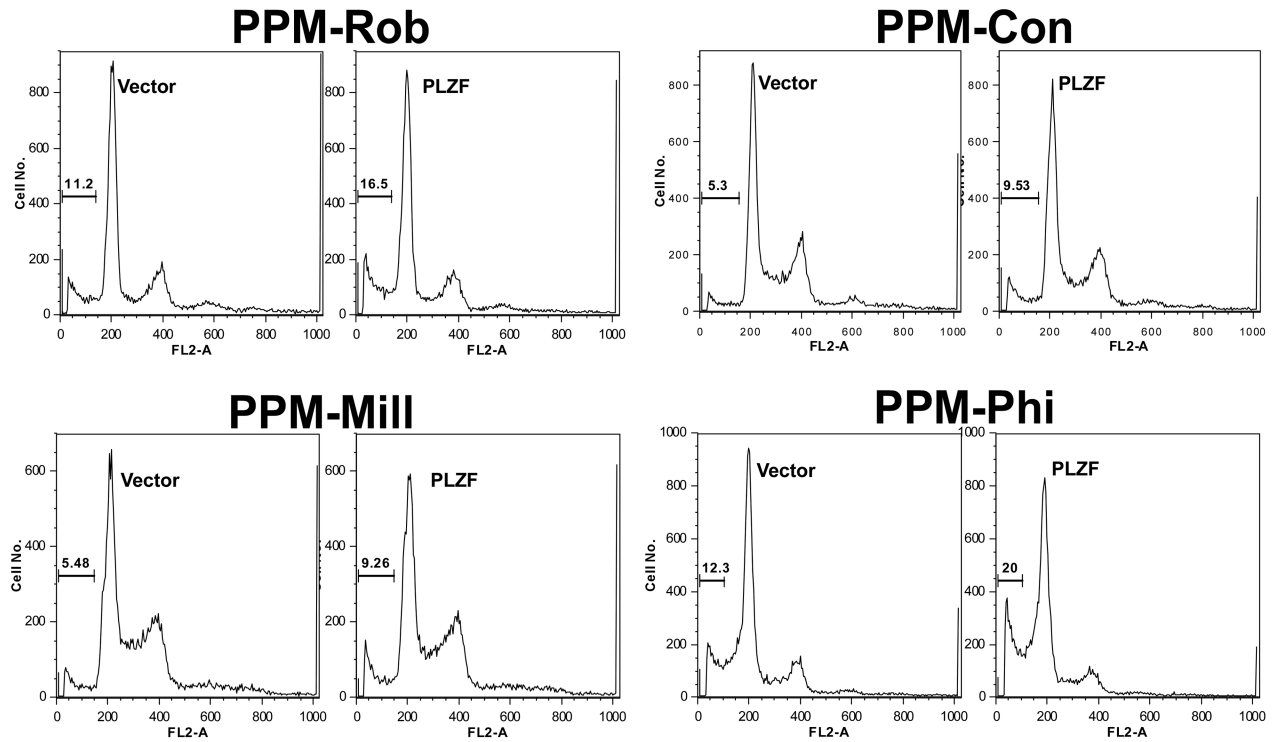
Figure 3.
Re-expression of PLZF in MM cells. *A)* Transfection of PLZF expression construct in four MM cell lines resulted in diminished cell proliferation, based on MTS assay 4 days after transfection using Amaxa Nucleofector. *B)* Representative clonogenic assay showing decreased colony formation in MM cells transfected with PLZF expression construct compared to cells transfected with empty vector. Cells were selected for 7 d in puromycin as described in the *Materials and Methods*. Quantitation of the clonogenic assays showed statistically significant differences (p < 0.05, 2-tailed Student t-test).

A

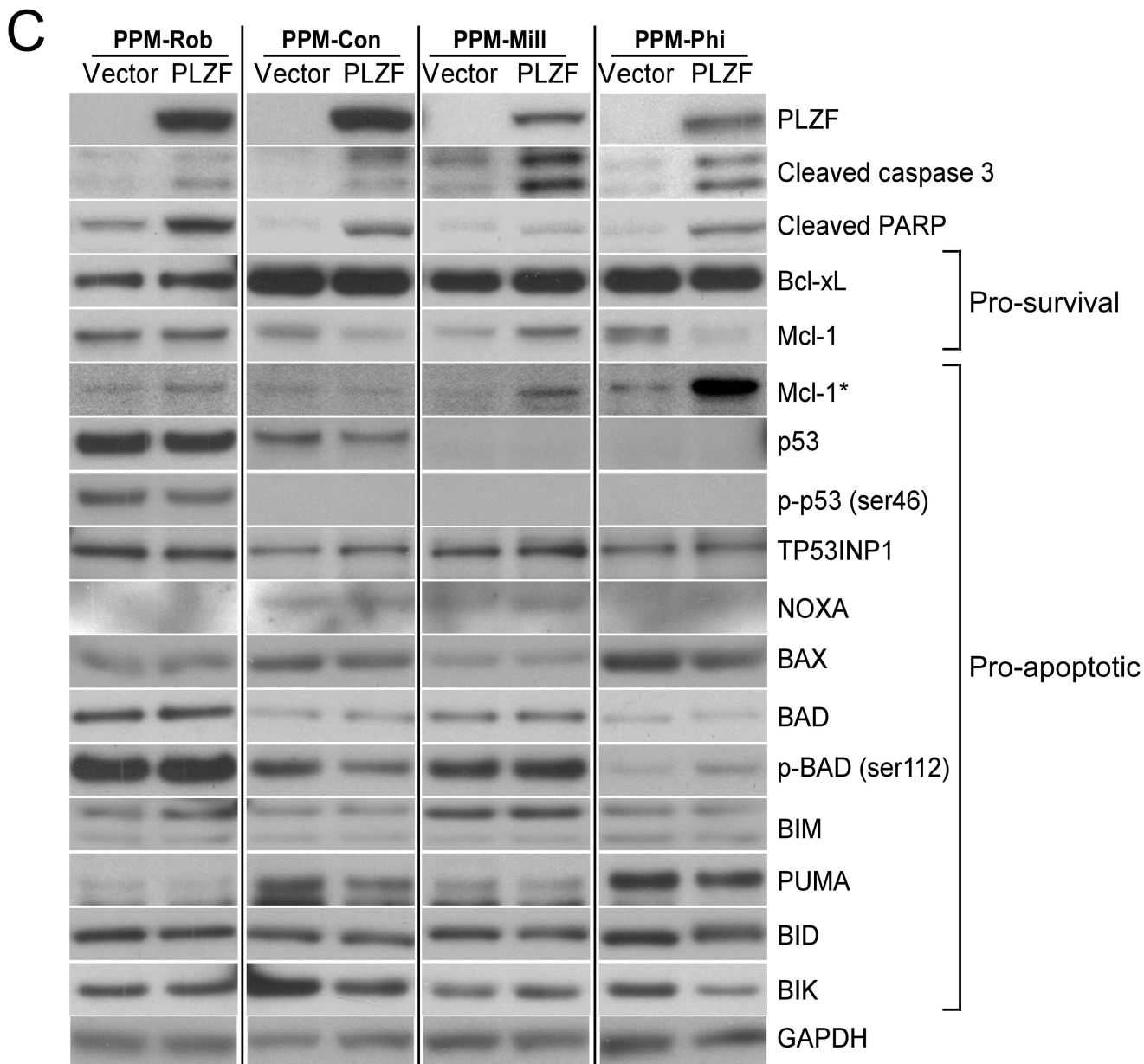
B

Figure 4.
PLZF re-expression in MM cells leads to increased apoptosis. *A)* Transfection of PLZF expression construct in four MM cell lines resulted in increased apoptosis, demonstrated by use of the Cell Death Detection ELISA plus assay 24 and 48 hours after transfection using Amaxa Nucleofector reagent. The results were statistically different ($p < 0.05$, 2-tailed Student t-test). *B)* Increase in sub-G1 percentage 48 hours after PLZF transfection. *C)* Western blot analysis demonstrating an increase in the pro-apoptotic Mcl-1 cleaved fragment (Mcl-1*) in MM cells transfected with PLZF expression construct compared to that observed in cells transfected with empty vector. Increased cleaved caspase-3 and cleaved PARP, indicative of increased apoptosis, were also observed. Immunoblotting for

other pro-apoptotic or pro-survival factors shown did not exhibit any consistent expression changes related to expression of PZLF. Cells were harvested 48 hours after transfection, and lysates were subjected to immunoblot analysis. Equal amounts (30 μg) of protein were subjected to SDS-PAGE, blotted, and incubated with various antibodies shown.